

© This manuscript version is made available under the CC-BY-NC-ND 4.0 license  
<https://creativecommons.org/licenses/by-nc-nd/4.0/>

The definitive publisher version is available online at  
<https://doi.org/10.1016/j.jmmm.2021.168602>

# Improvement on Parameter Identification of Modified Jiles-Atherton Model for Iron Loss Calculation

Pejush Chandra Sarker<sup>\*a</sup>, Youguang Guo<sup>a</sup>, Hai Yan Lu<sup>a</sup>, Jian Guo Zhu<sup>b</sup>

<sup>a</sup> Faculty of Engineering and Information Technology, University of Technology Sydney, Australia

<sup>b</sup> School of Electrical and Information Engineering, The University of Sydney, Australia

**Abstract:** The physical behaviour of a magnetic material can be characterized by Jiles-Atherton (J-A) model where some model parameters are generally identified by optimization techniques. For identification of model parameters using optimization techniques, an error criterion based on the error between measured and calculated magnetic flux density ( $B$ ) or magnetic field strength ( $H$ ) is commonly considered where the relative error in the calculation of iron loss is ignored. Consequently, the calculated iron loss from B-H loop sometimes highly differs from its experimental value. In this research, the relative iron loss error is also considered as optimization criterion along with the general existing error criterion. Furthermore, a modified J-A model is also proposed in order to improve the agreement between experimental and calculated results especially at the low magnetic induction levels by introducing a scaling factor in the anhysteretic magnetization. The proposed error criteria for parameter identification and proposed modified J-A model are tested by comparing the results with experimental and recently published works.

**Keywords**—Jiles-Atherton model; Fe-based amorphous magnetic material; Hysteresis and dynamic losses; Anhysteretic magnetization

## 1. Introduction

For design and analysis of electromagnetic devices such as transformer and inductors, the proper prediction of iron or core loss in their magnetic cores is essential as the iron loss is one of the heat sources in the devices. Therefore, the core loss modelling as well as other physical behaviour of the magnetic cores need to be investigated before designing electromagnetic devices [1]. Two types of models are generally utilized for modelling of magnetic cores. In the first type of modelling, the Steinmetz equation based empirical models [2, 3] are used for core loss prediction where the Steinmetz parameters are calculated by curve fitting of core loss data of material samples. In the empirical models, the core loss is mainly concerned but the other non-linear physical behaviour of the magnetic core is ignored. Finite element method (FEM) is commonly used for designing and analysing the electromagnetic devices. The main problem of the empirical models is that they cannot be directly incorporated into FEM as the prediction of the pattern of magnetic field strength ( $H$ ) from magnetic flux density ( $B$ ), which is one of the steps of the FEM analysis [4], is not possible using the empirical models. Therefore, for incorporation of magnetic properties of a magnetic material with FEM, a single value B-H curve is used along with the empirical models [5]. Since the complete physical behaviour of a magnetic material cannot be expressed by a single value B-H curve of the material, the actual results cannot be obtained from this approach [5].

On the other hand, in the second type of modelling the actual physical behaviours of the magnetic cores are considered, and the prediction of  $H$  from  $B$  or its vice versa are possible to be calculated. Preisach [6-8] and Jiles-Atherton (J-A) [9-12] models are generally utilized in this type of modelling. The problems of the Preisach model are that the model needs more computational time and memory resources compared to the J-A model [1, 13]. Consequently J-A model becomes popular and useful tools for characterization of magnetic materials [14]. Depending on the orientation of the magnetic field, two types of J-A models, such as scalar J-A model and vector J-A model [15], are used for characterization of a magnetic material. In this paper, the scalar J-A model, which is generally used for a fixed orientation, is considered to characterize a Fe-based amorphous magnetic material named amorphous 1k101 [16, 17] under alternating field that varies with time along a fixed orientation.

---

\*Corresponding author

Email: pejushchandra.sarker@student.uts.edu.au

The original J-A model consists of some equations where five parameters generally need to be identified which are pinning coefficient or loss factor  $k$ , reversibility coefficient  $c$ , domain interaction  $\alpha$ , anhysteretic magnetization's shape parameter  $a$ , and saturation magnetization  $M_s$  [9-12]. In the original J-A model [9-11], all model parameters are considered as constant for whole range of magnetic induction levels. Different researchers [1, 18] later observed that the pinning parameter or loss parameter  $k$  depends on the magnetic induction levels. After considering the loss factor as a function of  $B$  or  $H$ , the modelling of magnetic core shows higher agreement between measured and calculated waveform of  $B$  or  $H$  than that with the constant loss factor  $k$ . In the same way, it was also observed that at low magnetic induction levels, J-A model produces more error in calculation of core loss as well as higher difference between experimental and calculated waveform of  $B$  or  $H$  than those at high magnetic induction levels [19-21]. The main reason for high discrepancy at low magnetic induction levels is that model parameters are calculated based on a large B-H loop, and consequently the rate of reversible magnetizations at lower magnetic induction levels becomes larger than its actual values. To reduce the rate of the reversible magnetization a scaling factor, which can be a constant value or the function of  $B$  or  $H$  depending on the input of the model, is incorporated into the equation of rate of change of reversible magnetization [19-21]. Therefore, both calculated iron loss and calculated  $B$  or  $H$  show an improved agreement with experimental results. Recently authors of [5], considered both variable loss factor  $k$  and variable scaling factor  $R$  in the J-A model which gives higher agreement between experimental and calculated results than their constant values or one of them keeping constant and another variable.

The model parameters are initially calculated by solving some equations which are based on model equations at some specific conditions on a large B-H loop of a magnetic material [10, 11, 22]. The problem of the initial methods is that the methods provide low accuracy. Later different optimization techniques [18, 20, 23-25] such as genetic algorithm, stimulated annealing and particle swarm optimization are utilized to obtain the model parameters, which improve the accuracy of the J-A model. The optimization techniques as well as other similar methods [1, 12] are actually exploited in such a way that an error criterion becomes the minimum. The different error criteria [1, 12, 18, 23, 26, 27] such as the mean error, or mean square error or root mean square error between experimental and calculated  $B$  or  $H$  are generally used in the optimization techniques. However, among different error criteria, the root mean square is widely used to identify the model parameters. The identified model parameters are then used for calculation of B-H loop and the iron loss is finally calculated from the calculated B-H loop. The detailed analysis of measured and calculated B-H loop shows that the minimum relative error in the iron loss calculation does not often occur simultaneously with the minimum root mean square error of calculated  $B$  or  $H$ . It is also observed that with a slight increase of root mean square of error between calculated and measured waveform of  $B$  or  $H$ , the relative error of the calculation of iron loss reduces significantly. Therefore, in the optimization techniques double error criteria, where one is based on the conventional root mean square of error and the other based on the relative iron loss error, can be a good technique for high accuracy of iron loss calculation along with satisfactory calculated waveform of  $B$  or  $H$ . In this study, Brute Force algorithm-based optimization [28] is utilized to identify the model parameters. The advantages of the Brute Force optimization method are that the method is easily executed, and does not require derivative evaluation or any sophisticated intelligent techniques.

If the root mean square error of calculated  $B$  or  $H$  slightly increases, the error in the calculation of coercive magnetic force ( $H_c$ ) increases a little bit. To improve the calculation of  $H_c$  as well as  $B$  or  $H$ , the scaling factor can be included in the anhysteretic magnetization instead of its general inclusion into the equation of rate of change of reversible magnetization. The inclusion of scaling factor in the anhysteretic magnetization simultaneously reduces the rate of irreversible magnetization and anhysteretic magnetization, and consequently it provides better agreement between experimental and simulated results than the existing inclusion way of scaling factor.

In this paper, a Fe-based amorphous magnetic material is characterized by modified J-A model. The main contributions of the research include incorporation of an additional error criterion along with general error criterion for the identification of the J-A model parameters, and inclusion of scaling factor in the anhysteretic magnetization of original J-A model in order to reduce the rate of irreversible magnetization and anhysteretic magnetization especially at the low magnetic induction level. Dynamic models which signifies the eddy current and excess loss models are later incorporated with the static modified J-A model to make the model generalized. The proposed method of parameter identification and proposed modified J-A model are examined by comparing the calculated results with experimental as well as recently published modified J-A model works.

## 2. Review of J-A model

According to the J-A model [10, 11], the magnetization is considered as a sum of irreversible ( $M_{irr}$ ) and reversible ( $M_{rev}$ ) magnetization which is expressed as follows:

$$M = M_{irr} + M_{rev} \quad (1)$$

with

$$M_{irr} = M_{an} - k\delta \frac{dM_{irr}}{dH_e} \quad (2)$$

$$M_{rev} = c(M_{an} - M_{irr}) \quad (3)$$

where  $k$  and  $c$  are the model parameters,  $M_{an}$  the anhysteretic magnetization,  $H_e$  the effective magnetic field strength and  $\delta$  the directional parameter which is +1 for  $dH/dt > 0$  and -1 for  $dH/dt < 0$ . The anhysteretic magnetization and the effective magnetic field strength can be expressed as follows [4]:

$$M_{an} = M_s \left[ \coth \frac{H_e}{a} - \frac{a}{H_e} \right] \quad (4)$$

$$H_e = H + \alpha M \quad (5)$$

where  $M_s$  is the saturation magnetization,  $M$  the total magnetization,  $H$  the applied magnetic field strength, and  $a$  and  $\alpha$  are the model parameters. In J-A model, the magnetization in the next time step is calculated from its present magnetization and its derivative with respect to the magnetic field strength ( $dM/dH$ ), and magnetic flux density  $B$  is then calculated from  $M$  and  $H$  [4], which are expressed as follows:

$$M(t + \Delta t) = M(t) + \frac{dM}{dH} \Delta H \quad (6)$$

$$B(t + \Delta t) = \mu_0 \{ H(t + \Delta t) + M(t + \Delta t) \} \quad (7)$$

According to the J-A model [11],  $dM/dH$  is obtained as follows:

$$\frac{dM}{dH} = (1-c) \frac{M_{an} - M_{irr}}{k\delta - \alpha(M_{an} - M_{irr})} + c \frac{dM_{an}}{dH} \quad (8)$$

Using the above-mentioned expressions of  $M_{irr}$ ,  $M_{rev}$ ,  $M_{an}$  and  $H_e$ , the total magnetization susceptibility ( $dM/dH$ ) can also be obtained by (9), which is expressed as follows [22]:

$$\frac{dM}{dH} = \frac{(1-c) \frac{dM_{irr}}{dH_e} + c \frac{dM_{an}}{dH_e}}{1 - \alpha(1-c) \frac{dM_{irr}}{dH_e} - \alpha c \frac{dM_{an}}{dH_e}} \quad (9)$$

where  $dM_{irr}/dH_e$  and  $dM_{an}/dH_e$  can be obtained from (2) and (4) respectively. From (2), the  $dM_{irr}/dH_e$  can be written as

$$\frac{dM_{irr}}{dH_e} = \frac{(M_{an} - M_{irr})}{k\delta} \quad (10)$$

It was reported in [11] and [15] that domain wall displacement does not exist if  $(M_{an} - M_{irr})dH_e < 0$  and in that case  $dM_{irr}/dH_e$  becomes zero. Therefore, (10) can be updated as follows [12, 15, 29]:

$$\frac{dM_{irr}}{dH_e} = \frac{\delta_M (M_{an} - M_{irr})}{k\delta} \quad (11)$$

where  $\delta_M$  is 1 if  $(M_{an} - M_{irr})dH_e > 0$ , and 0 if  $(M_{an} - M_{irr})dH_e \leq 0$ . From (1) and (3), the irreversible magnetization,  $M_{irr}$  can be calculated as follows:

$$M_{irr} = \frac{M - cM_{an}}{1 - c}. \quad (12)$$

However, it is reported in [1] and [18] that the pinning parameter of the J-A model changes with the magnetic induction levels. Therefore,  $k$  is considered as the function of  $H$  in [1] and [18], which improves the accuracy of the model. It is also observed in [19–21] that at low magnetic induction levels, the high discrepancy in the iron loss and  $B$  calculations occur in the J-A model. To reduce this problem, a scaling factor is included in (10) so that it limits the rate of irreversible magnetization especially at the low induction levels. According to [21], (10) can be modified as follows:

$$\frac{dM_{irr}}{dH_e} = \frac{(M_{an} - RM_{irr})}{k\delta} \quad (13)$$

where  $R$  is the scaling factor which can be expressed by the magnetic field strength or magnetic flux density depending on the input of the J-A model. Recently, the authors of [5] considered both the pinning coefficient  $k$  and scaling factor  $R$  as functions of peak magnetic field strength for inner loops. Therefore, for inner loops especially at low magnetic induction levels, the relative error in the calculation of iron loss reduces.

Identification of the model parameters are also important in the J-A model. Initially few equations corresponding to the model parameters are developed using model equations and a large B-H loop of a magnetic material [10, 11, 22]. Those equations are then solved numerically to obtain the J-A model parameters. In the last few decades, different optimization techniques were considered to obtain the J-A model parameters where an error criterion is generally set [12, 18, 23, 26, 27]. An error criterion which is based on the root mean square of the difference between measured and calculated magnetic flux density is commonly used in the optimization methods that can be expressed as follows [1]:

$$\varepsilon_s = \sqrt{\frac{\sum_i^N (B_{meai} - B_{cali})^2}{N}} \quad (14)$$

where  $\varepsilon_s$  is the root mean square of error,  $N$  the number of samples per period of the magnetic flux density,  $B_{meai}$  the measured magnetic flux density and  $B_{cali}$  the calculated magnetic flux density. After calculating the model parameters, the iron loss of the corresponding magnetic core is calculated as follows:

$$P = \frac{1}{T\rho} \int_T H \frac{dB}{dt} dt \quad (15)$$

where  $P$  is the iron loss (W/kg),  $T$  time period (s) and  $\rho$  the mass density ( $\text{kg/m}^3$ ) of the core. The error in the calculation of the iron loss is then obtained from difference between measured and calculated results which can be expressed as follows:

$$\varepsilon_r = \left| \frac{P_{mea} - P_{cal}}{P_{mea}} \right| \times 100\% \quad (16)$$

where  $\varepsilon_r$  is the relative iron loss error,  $P_{mea}$  is the measured iron loss and  $P_{cal}$  is the calculated iron loss.

### 3. Proposed model

In this research, it is investigated using experimental and calculated data that there exist some cases where the minimum root mean square of error ( $\varepsilon_s$ ) between calculated and measured  $B$ , and the minimum relative error in the iron loss calculation do not often occur simultaneously. Therefore, the relative error of iron loss calculation sometimes increases to maintain the minimum  $\varepsilon_s$ . The existing modified J-A model reported in [5] is firstly exploited here where  $k$  and  $R$  are assumed as function of  $H$ . After implementing the J-A model, it is observed from Fig. 1(a), that the minimum  $\varepsilon_s$  at 1.26 T is 0.0347 where the relative error of iron loss calculation,  $\varepsilon_r$  is 11.701%. On the other hand, the minimum relative error of the iron loss calculation at the same magnetic induction is 0.017% where the  $\varepsilon_s$  is 0.0625. Similarly, at 0.83 T, both types of errors do not occur simultaneously as shown in Fig. 1(b). It is observed from the calculated results that slight increase of  $\varepsilon_s$ , such as from 0.0347 to 0.0473 at 1.26 T, significantly reduces the iron loss error such as from 11.701% to 4.512%. Therefore, in this research both  $\varepsilon_s$  and  $\varepsilon_r$  are considered as error criteria where both are slightly higher than their minimum values, i.e. a trade-off between  $\varepsilon_s$  and  $\varepsilon_r$  is set as error criteria in the optimization technique. To express  $\varepsilon_s$  as percentage of its maximum value, (14) can be updated as follows:

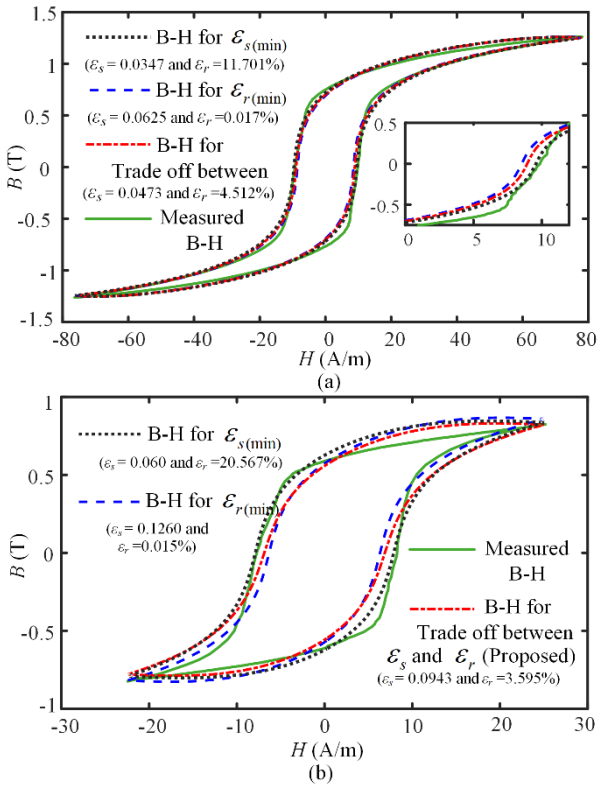


Fig. 1. Comparison of B-H loops obtained from measured and J-A models under 1 Hz sinusoidal excitation at (a)  $B_m = 1.26$  T and (b)  $B_m = 0.83$  T.

$$\varepsilon_s = \frac{1}{\max(B_{meai})} \sqrt{\sum_i^N \frac{(B_{meai} - B_{cali})^2}{N}} \times 100\% . \quad (17)$$

Since  $\varepsilon_s$  slightly increases by the proposed parameter identification method, the errors of the calculation of coercive magnetic field strengths ( $H_c$ ) increases as shown in Fig. 2. To mitigate these errors, the rate of irreversible component can be reduced especially at lower magnetic induction levels by introducing scaling factor in the anhysteretic magnetization as shown in (18) instead of the scaling factor with the irreversible component of magnetization [5] as shown in (13). Therefore, according to the proposed anhysteretic magnetization, the expressions of the anhysteretic magnetization and its derivative with respect to  $H_c$  can be written as:

$$M_{an} = \nu M_s \left[ \coth \frac{H_e}{a} - \frac{a}{H_e} \right] \quad (18)$$

$$\frac{M_{an}}{dH_e} = \frac{\nu M_s}{a} \left[ 1 - \coth^2 \left( \frac{H_e}{a} \right) + \left( \frac{H_e}{a} \right)^2 \right] \quad (19)$$

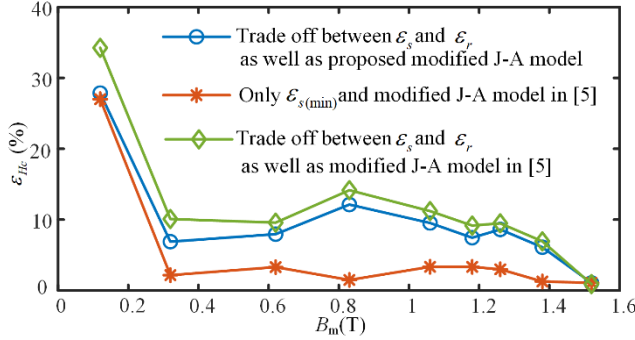


Fig. 2. The percentage of error in the calculation of coercive magnetic field strength,  $\epsilon_{Hc}$  with the change of peak magnetic flux densities.

where  $\nu$  is the scaling factor which is the function of  $H$  or  $B$  depending on the input of J-A model. As the scaling factor is only necessary for inner B-H loops, the parameter identification for the large B-H loop is carried out with considering 1 as the value of  $\nu$ . Since domain wall displacement does not exist in some specific condition, e.g.  $(M_{an} - M_{irr})dH_e < 0$ , the rate of irreversible magnetization with respect to the  $H_e$  in this research is calculated by (11) instead of (13).

To identify the J-A model parameters, a large B-H loop with different inner loops are firstly experimentally measured, as the identification process is based on the measured data. The detailed experimental process is discussed in [8]. Since Brute Force optimization technique is utilized in this study, according to the technique the J-A model parameters ( $k$ ,  $c$ ,  $a$ ,  $\alpha$  and  $M_s$ ) are swept away over their specific ranges to produce many sets of model parameters. After that J-A model is implemented using each set of model parameters to calculate  $B$  from a given  $H$  of a large measured B-H loop. The calculated and measured B-H loops are then exploited to calculate the objective functions which are: (i)  $\epsilon_r < \epsilon_{rc}$  and (ii)  $\epsilon_s < \epsilon_{sc}$ , where  $\epsilon_{rc}$  and  $\epsilon_{sc}$  are minimum allowable  $\epsilon_r$  and  $\epsilon_s$  respectively, and  $\epsilon_r$  and  $\epsilon_s$  are calculated by (16) and (17) respectively. If the values of  $\epsilon_r$  and  $\epsilon_s$  remain within their limits, their values and corresponding model parameters are stored otherwise rejected them. When the search is completed, the required solution is selected from the stored data depending on the optimal target. After selection of J-A model parameters for the large loop, the variables  $k$  and  $\nu$  at other induction levels are calculated with considering other selected four parameters ( $c$ ,  $a$ ,  $\alpha$  and  $M_s$ ) as constant. In these cases,  $k$  and  $\nu$  are only swept away over their ranges, and their optimum values are selected as the same way as for the large B-H loop. Fig. 3 shows the flow chart of proposed method for identification of J-A model parameters. However, instead of a single global optimum value, a set of optimal solutions which is called as Pareto-optimal solutions is generally obtained in this study. Pareto-optimal solutions for calculation of  $k$  and  $\nu$  at 1.26 T is shown in Fig. 4. From the Fig. 4, it is observed that minimum  $\epsilon_r$  and  $\epsilon_s$  do not occur at the same point where each point associates with a feasible set of  $k$  and  $\nu$  that satisfy the error criteria. Thus, a point is selected in such a way that both  $\epsilon_r$  and  $\epsilon_s$  remain in the acceptable values as shown in the Fig. 4.

The selected constant parameters  $c$ ,  $a$ ,  $\alpha$  and  $M_s$  of the J-A model are shown in Table 1. The values of  $k$  and  $\nu$  for the considered magnetic core are shown in Figs. 5 and 6 respectively.

In the above proposed algorithm of the J-A model parameter identification, one of the important tasks is calculation of  $B$  from  $H$  using J-A model as shown in Fig. 3. For implementation of J-A model,  $H_e$ ,  $M_{an}$ ,  $dM_{an}/dH_e$ ,  $M_{irr}$  and  $dM_{irr}/dH_e$  are firstly calculated by (5), (18), (19), (12), and (11) respectively. After that the calculated values of  $dM_{an}/dH_e$  and  $dM_{irr}/dH_e$  are exploited to calculate the value of  $dM/dH$  by (9). The value of  $dM/dH$  at any time step is used to calculate the magnetization for next time step by (6). Finally, the corresponding  $B$  for a given  $H$  is calculated by (7). The process is repeated until the calculation of  $B$  for all given time steps is finished.

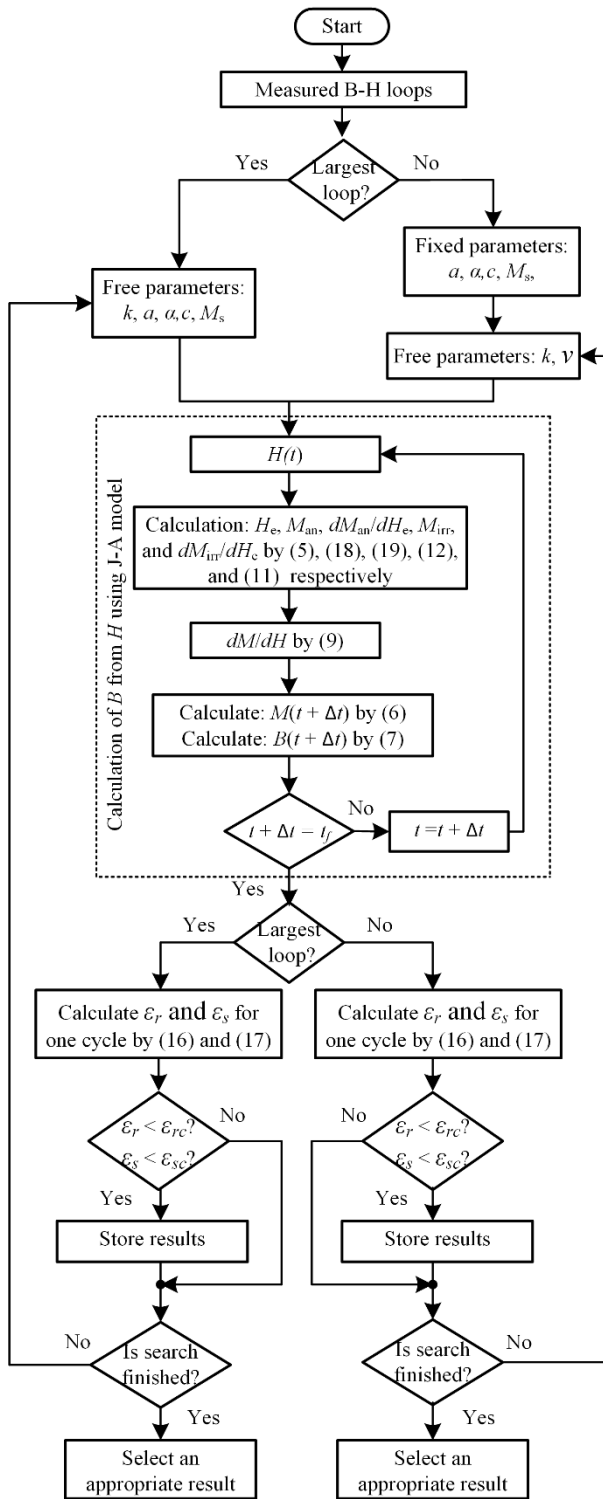


Fig. 3. Flow chart of proposed method for the identification of J-A model parameters.



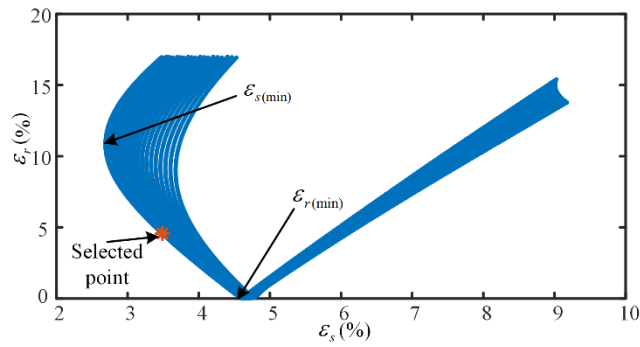


Fig. 4. Pareto-optimal solutions by optimization technique to identify model parameters at 1.26 T.

Table 1

The selected values of J-A model parameters

J-A model parameters	Selected value
$c$	0.18
$a$	53.51 A/m
$\alpha$	$1.10 \times 10^{-5}$
$M_s$	1420000 A/m

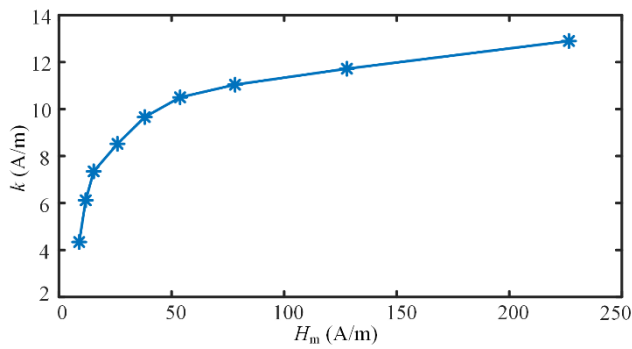


Fig. 5. The values of the loss factor  $k$  with the change of peak magnetic field strength,  $H_m$ .

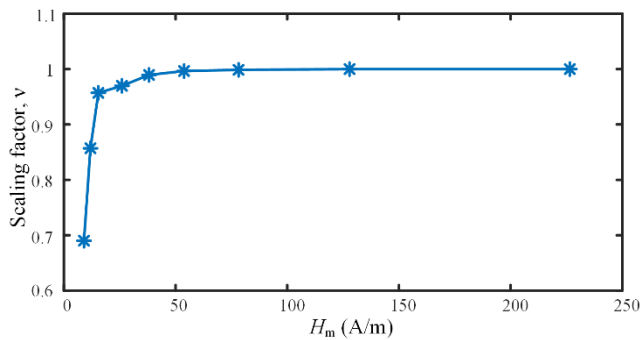


Fig. 6. The values of scaling factor  $\nu$  with the change of peak magnetic field strength,  $H_m$ .

#### 4. Inverse J-A model

For modelling of a magnetic material using finite element method, it is necessary for calculation of  $H$  from  $B$  which can be achieved by inverse J-A model. In the inverse J-A model, the calculation  $M$  at the next time step is firstly carried out using its present value, its derivative with respect to  $B$  ( $dM/dB$ ) and the change of  $B$  between two consequent steps as the same as the direct J-A model [21]. Finally,  $H$  is calculated from  $M$  and  $B$ . Using the

modified J-A model, the change of magnetization with respect to magnetic flux density can be defined by as follows [29]:

$$\frac{dM}{dB} = \frac{(1-c)\delta_M (M_{an} - M_{irr}) + k\delta c \frac{dM_{an}}{dH_e}}{\mu_0 \left[ k\delta - (\alpha-1)(1-c)\delta_M (M_{an} - M_{irr}) - (\alpha-1)k\delta c \frac{dM_{an}}{dH_e} \right]} \quad (20)$$

where  $M_{an}$  in this research is calculated by (18) instead of conventional  $M_{an}$  as shown in (4), and  $dM_{an}/dH_e$  is correspondingly calculated by (19). Similar to the proposed modified J-A model,  $k$  and  $\nu$  are considered as variables in the proposed modified inverse J-A model. The same values of other constant parameters of the J-A model are used in the inverse J-A model. The values of  $k$  and  $\nu$  of inverse J-A model are also calculated as the same as the proposed modified J-A model. Figs. 7 and 8 show the obtained values of  $k$  and  $\nu$  with the change of peak magnetic flux density, respectively.

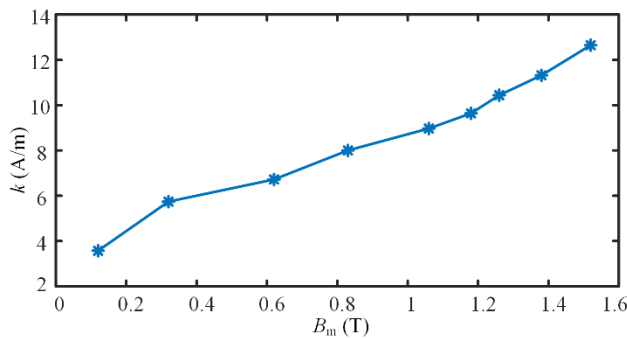


Fig. 7. The values of the loss factor  $k$  with the change of peak magnetic flux density,  $B_m$ .

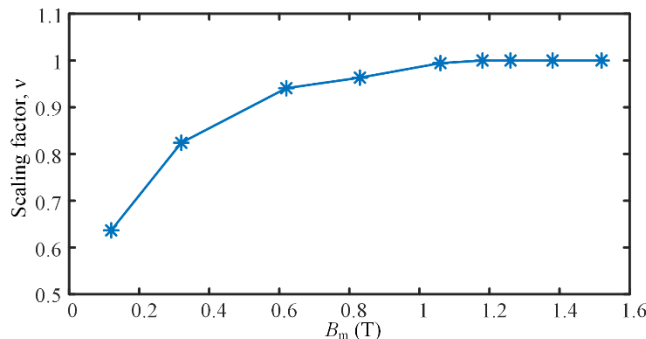


Fig. 8. The values of scaling factor  $\nu$  with the change of peak magnetic flux density,  $B_m$ .

## 5. Inclusion of dynamic losses

Both direct and inverse J-A models with certain model parameters can be used for any specific frequency where all types of magnetic iron losses, e.g. hysteresis loss, eddy current and excess losses, are inherently retained there. The same J-A parameters cannot be applied if the operating frequency is changed as the B-H loop changes with the frequency. To make the generalized J-A model, loss separation approach is considered in this study where hysteresis, eddy current and excess losses are modelled separately [4]. The magnetic field strength corresponding to the hysteresis loss is calculated using inverse J-A model, and the magnetic field strengths corresponding to other two losses are calculated from the classical eddy current and excess loss models. For hysteresis loss, parameter identification of the inverse J-A model can be carried out based on the B-H loops at very low frequency (no more than 1 Hz) as at that low operating frequency the eddy current and excess loss are negligible. The obtained model parameters can be then used for calculating hysteresis loss and corresponding magnetic field strength for any frequency. Therefore, the total magnetic field strength can be written as [4, 30]:

$$H_T = H + \frac{\sigma d^2}{12} \frac{\Delta B}{\Delta t} + (\sigma G V_0 A_l)^{1/2} \frac{\Delta B}{\Delta t^{0.5} |\Delta B|^{0.5}} \quad (21)$$

where  $H_T$  is the total magnetic field strength,  $d$  thickness of the amorphous ribbon,  $\sigma$  conductivity,  $\Delta t$  the time step between two samples,  $\Delta B$  the change of magnetic flux density within  $\Delta t$ ,  $A_l$  the cross-sectional area of the magnetic material sheet or ribbon, and  $G$  and  $V_0$  are constant coefficients. The  $(\sigma G V_0 A_l)^{1/2}$  in (21) can be calculated by using curve fitting of core loss data which can be obtained in details in [8, 30, 31]. The total iron loss is then calculated by (15) where the total magnetic field strength is calculated by (21).

## 6. Result and discussion

For experimental verification of the proposed error criteria and proposed modified J-A model, a toroidal amorphous magnetic core is utilized in this research. The details of experimental procedure can be obtained in [8].

It has been already discussed in Section 3 that the minimum  $\varepsilon_s$  and minimum  $\varepsilon_r$  do not often occur simultaneously, and consequently the relative iron loss error  $\varepsilon_r$  at minimum  $\varepsilon_s$  sometimes becomes much higher than its minimum value. Therefore, by using the proposed error criteria where two error criteria are exploited, the value of  $\varepsilon_r$  reduces significantly as shown in Fig. 9. On the contrary, the proposed error criteria of optimization methods for parameter identification slightly increases the values of  $\varepsilon_s$  as shown in Fig. 10. However, the proposed modified J-A model, where scaling factor is introduced in the anhysteretic magnetization, reduces the percentage of root mean square error  $\varepsilon_s$  as shown in Fig. 10. In addition, the proposed modified J-A model reduces the error in the calculation of coercive magnetic forces as shown in Fig. 2 (Section 3). From Fig. 10 it is also observed that the  $\varepsilon_s$  for the J-A models decreases significantly with the increase of the magnetic induction level. At low magnetic induction level such as 0.12 T, the  $\varepsilon_s$  for the proposed modified J-A model is about 19.59 %. On the other hand, at high induction level such as 1.52 T, the  $\varepsilon_s$  is about 1.92 %.

It is observed from Fig. 1(b), the measured B-H loops becomes slightly asymmetric at low induction level. Consequently, its corresponding calculated B-H loops become asymmetric a little bit. The measured B-H loop slightly shifts along the magnetic field axis due to the effect of exchange bias during the magnetization process [32, 33]. In addition, due to intrinsic drawbacks of J-A model, the calculated B-H loop at low magnetic induction become somewhat asymmetric.

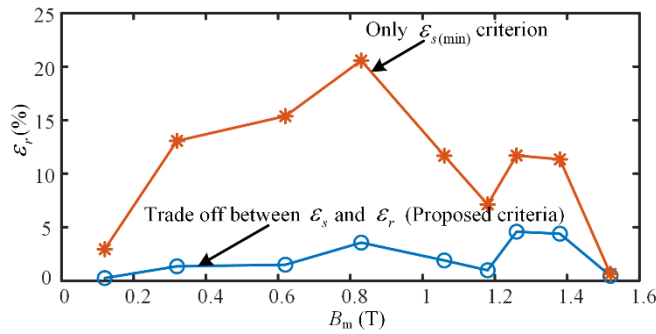


Fig. 9. Percentage of core loss error,  $\varepsilon_r$  with change of peak magnetic flux densities for the proposed error criterion and existing error criterion.

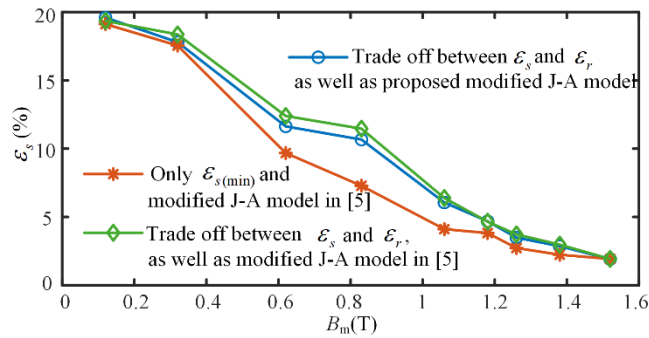


Fig. 10. Percentage of root mean square errors in the calculation of  $B$  at different peak magnetic flux densities under different condition of J-A models.

In this research, the inverse J-A model is also based on the proposed error criteria and proposed modified J-A model. As  $H$  is calculated from  $B$  for the inverse J-A model, both loss factor and scaling factor depends on the  $B_m$ . From Fig. 11 it is observed that the calculated  $H$  using proposed modified inverse J-A model shows a strong agreement with the measured  $H$ , where the correlation coefficient,  $r$  is 0.9987. For consideration of more complex signals than conventional sinusoidal signal, the minor loops loop over a major B-H loop is considered in this research. Two minor loops over a major B-H loop is experimentally obtained by applying an excitation voltage which consists of a 1 Hz fundamental sinusoidal component with a third harmonic component [8]. Proposed modified inverse J-A model is then applied to calculate the B-H loop. Fig. 12 shows the comparison between the experimental and calculated B-H loops. From the Fig. 12, it is observed that the calculated minor loops become slightly bigger than the calculated ones and consequently, the error in the calculated core loss ( $\epsilon_r=8.31\%$ ) increases a little bit. The reversible magnetization is mainly responsible for minor loops. Consequently, the value of reversibility coefficient  $c$  needs to be high for minor loop. Since the constant value of  $c$  is considered for major and minor loops, the mismatch between calculation of core loss increases slightly. In this case, the correlation coefficient between measured and calculated  $H$  is 0.9948.

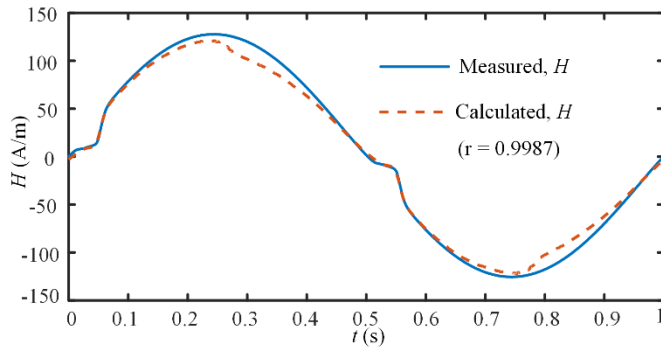


Fig. 11. Comparison between calculated and measured  $H$  at  $B_m=1.38$  T and 1 Hz excitation.

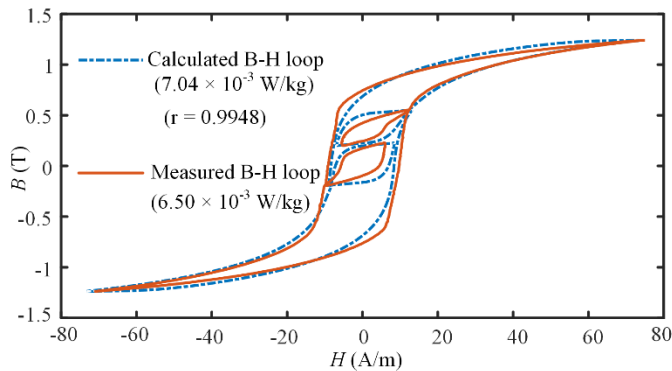


Fig. 12. Comparison between calculated and measured B-H loop for minor loops over a major loop.

To observe the effect of hysteresis, eddy current and excess loss effects on the total core loss, the core loss is measured at 1.08 T at different frequencies. After that the inverse J-A model along with eddy current and excess models are exploited, and their results are graphically presented in Fig. 13. It is observed from Fig. 13 that hysteresis loss per frequency is almost constant with the increase of frequency. On the other hand, both eddy current and excess losses increase with the frequency although the effect of eddy current is very small compared to the other two losses due to the very thin amorphous ribbon. It is also seen from Fig. 13 that the calculated total core loss is very close to the measured ones.

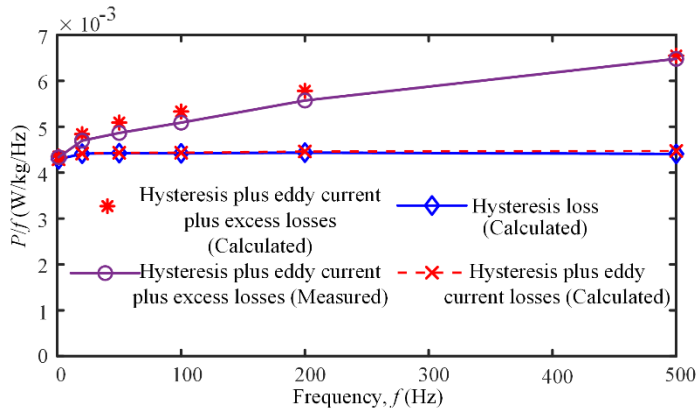


Fig. 13. Core loss separation using proposed modified inverse J-A model.

Fig. 14 shows the measured and calculated B-H loops with the inclusion of dynamic core loss model with the inverse J-A model. It is observed from Fig. 14 that calculated B-H loops under 500 Hz excitation at 1.41 T and 0.67 T are close to their measured ones where the correlation coefficients in the calculation of  $H$  are 0.9973 and 0.9603 respectively. The relative error in the iron loss calculation,  $\epsilon_r$  for these two cases are 2.86% and 0.16%, whereas  $\epsilon_s$  are 3.46% and 16.13% respectively. It is seen from Fig. 15 that the calculated iron loss results show a strong agreement with the measured results for whole range of magnetic induction where the correlation coefficient among their results is 0.9998.

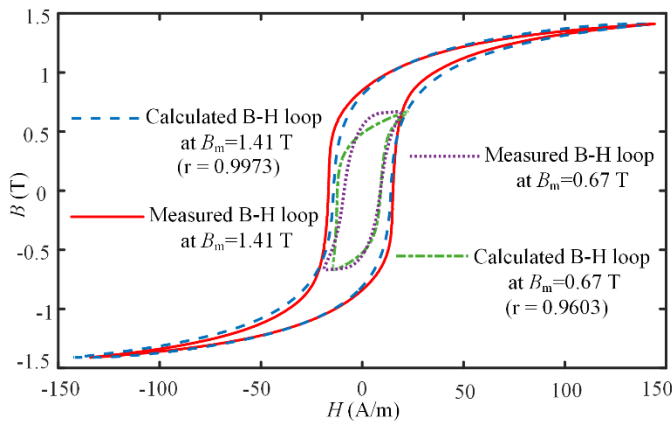


Fig. 14. Comparison between measured and calculated B-H loops at 1.41 T and 0.67 T under 500 Hz excitation.

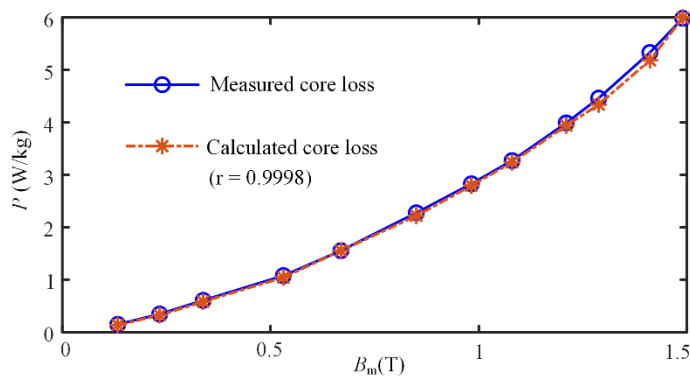


Fig. 15. Comparison between measured and calculated core loss at 500 Hz with different peak magnetic flux densities.

## 7. Conclusion

In this paper, two error criteria instead of conventional one error criterion are proposed in the optimization method, where one is based on the conventional root mean square of error and the other based on the relative error of iron loss. The proposed error criteria for parameter identification significantly reduce the error of iron loss calculation e.g., at 1.26 T the iron loss error reduces from 11.701% to 4.512%. A proposed modified J-A model, where a scaling factor is incorporated with anhysteretic magnetization, along with the projected parameter identification technique reduces the value of the root mean square of error between the measured and calculated waveform. The proposed modified model also improves the calculation of coercive magnetic force e.g., the error in calculation of  $H_c$  at 0.62 T reduces from 9.58% to 7.95%. The inverse J-A model based on the proposed modified J-A model also provides good results for both sinusoidal and non-sinusoidal excitations. With the inclusion of dynamic core loss model with the modified inverse J-A model, there exists strong agreement between calculated and measured iron losses at different frequency and magnetic induction levels, e.g. the error of iron loss calculation under 500 Hz sinusoidal excitation at 0.67 T and 1.28 T is 0.16% and 2.86%, respectively.

## Reference

- [1] M. Toman, G. Stumberger, D. Dolinar, Parameter identification of the Jiles–Atherton hysteresis model using differential evolution, *IEEE Trans. Magn.* 44 (6) (2008) 1098–1101.
- [2] I. Villar, U. Viscarret, I. Etxeberria-Otadui, A. Rufer, Global loss evaluation methods for nonsinusoidally fed medium-frequency power transformers, *IEEE Trans. Ind. Electron.* 56 (10) (2009) 4132–4140.
- [3] P. C. Sarker, M. R. Islam, Y. Guo, J. Zhu, H. Y. Lu, State-of-the-art technologies for development of high frequency transformers with advanced magnetic materials, *IEEE Trans. Appl. Supercond.* 29 (2) (2019) 7000111.
- [4] N. Sadowski, N. J. Batistela, J. P. A. Bastos, M. Lajoie-Mazenc, An inverse Jiles–Atherton model to take into account hysteresis in time-stepping finite-element calculations, *IEEE Trans. Magn.* 38 (2) (2002) 797–800.
- [5] S. Hussain, D. A. Lowther, The Modified Jiles–Atherton Model for the accurate prediction of iron losses, *IEEE Trans. Magn.* 53 (6) (2017) 7300504.
- [6] I. D. Mayergoyz, Dynamic Preisach models of hysteresis, *IEEE Trans. Magn.* 24 (6) (1988) 2925–2927.
- [7] S. R. Naidu, Simulation of the hysteresis phenomenon using Preisach’s theory, *IEE Proc. A Phys. Sci. Meas. Instrum. Man. Educ.* 137 (2) (1990) 73–79.
- [8] P. C. Sarker, Y. Guo, H. Y. Lu, J. G. Zhu, A generalized inverse Preisach dynamic hysteresis model of Fe-based amorphous magnetic materials, *J. Magn. Magn. Mater.* 514 (2020) 167290.
- [9] D. C. Jiles, D. L. Atherton, Theory of ferromagnetic hysteresis, *J. Magn. Magn. Mater.* 61 (1–2) (1986) 48–60.
- [10] D. C. Jiles, J. B. Tholke, Theory of ferromagnetic hysteresis: determination of model parameters from experimental hysteresis loops, *IEEE Trans. Magn.* 25 (5) (1989) 3928–3930.
- [11] D. C. Jiles, J. B. Tholke, M. K. Devine, Numerical determination of hysteresis parameters for the modeling of magnetic properties using the theory of ferromagnetic hysteresis, *IEEE Trans. Magn.* 28 (1) (1992) 27–35.
- [12] P. Kis, A. Iványi, Parameter identification of Jiles–Atherton model with nonlinear least-square method, *Phys. B: Cond. Mat.* 343 (1–4) (2004) 59–64.
- [13] S. Rosenbaum, M. Ruderman, T. Strohmaier, T. Bertram, Use of Jiles–Atherton and preisach hysteresis models for inverse feed-forward control, *IEEE Trans. Magn.* 46 (12) (2010) 3984–3989.
- [14] Z. Birčáková, P. Kollár, J. Füzér, R. Bureš, M. Fáberová, Magnetic properties of selected Fe-based soft magnetic composites interpreted in terms of Jiles–Atherton model parameters, *J. Magn. Magn. Mater.* 502 (2020) 166514.
- [15] A. J. Bergqvist, A simple vector generalization of the Jiles–Atherton model of hysteresis, *IEEE Trans. Magn.* 32 (5) (1996) 4213–4215.
- [16] Henan ZY Amorphous Technology Co. Ltd. [Online]. Available: <https://www.zyamorphous.com/>. (Accessed 25 November 2020).
- [17] Guangzhou Amorphous Electronic Technology Co. Ltd., Guangzhou, China. [Online]. Available: <https://coilcore.en.alibaba.com/>. (Accessed 22 December 2020).

- [18] P. R. Wilson, J. N. Ross, A. D. Brown, Optimizing the Jiles-Atherton model of hysteresis by a genetic algorithm, *IEEE Trans. Magn.* 37 (2) (2001) 989–993.
- [19] K. H. Carpenter, A differential equation approach to minor loops in the Jiles-Atherton hysteresis model, *IEEE Trans. Magn.* 27 (6) (1991) 4404–4406.
- [20] D. Lederer, H. Igarashi, A. Kost, and T. Honma, On the parameter identification and application of the Jiles-Atherton hysteresis model for numerical modelling of measured characteristics, *IEEE Trans. Magn.* 35 (3) (1999) 1211–1214.
- [21] J. V. Leite, A. Benabou, N. Sadowski, Accurate minor loops calculation with a modified Jiles-Atherton hysteresis model, *COMPEL-Int. J. Comput. Math. Elect. Electron. Eng.* 28 (3) (2009) 741–749.
- [22] J. P. A. Bastosa, N. Sadowski, *Electromagnetic modeling by finite element methods*, Boca Raton, FL: CRC Press (2003) 438–455.
- [23] I. Podbereznyaya, A. Pavlenko, Accounting for dynamic losses in the Jiles-Atherton model of magnetic hysteresis, *J. Magn. Magn. Mater.* 513 (2020) 167070.
- [24] Y. Li, J. Zhu, Yongjian Li, H. Wang, L. Zhu, Modeling dynamic magnetostriction of amorphous core materials based on Jiles–Atherton theory for finite element simulations, *J. Magn. Magn. Mater.* 529 (2021) 167854.
- [25] F. R. Fulginei, A. Salvini, Softcomputing for the identification of the Jiles-Atherton model parameters, *IEEE Trans. Magn.* 41 (3) (2005) 1100–1108.
- [26] D. Zhang, M. Jia, Y. Liu, Z. Ren, C. Koh, Comprehensive improvement of temperature-dependent Jiles–Atherton model utilizing variable model parameters, *IEEE Trans. Magn.* 54 (3) (2018) 7300504.
- [27] J. V. Leite, N. Sadowski, P. Kuo-Peng, N. J. Batistela, J. P. A. Bastos, The inverse Jiles-Atherton model parameters identification, *IEEE Trans. Magn.* 39 (3) (2003) 1397–1400.
- [28] M. Mahoor, F. R. Salmasi, and T. A. Najafabadi, "A hierarchical smart street lighting system with Brute-Force energy optimization," *IEEE Sens. J.* 17 (9) (2017) 2871–2879.
- [29] W. Li, I. H. Kim, S. M. Jang, C. S. Koh, Hysteresis modeling for electrical steel sheets using improved vector Jiles-Atherton hysteresis model, *IEEE Trans. Magn.* 47 (10) (2011) 3821–3824.
- [30] E. Fallah, J. S. Moghani, A new approach for finite-element modeling of hysteresis and dynamic effects, *IEEE Trans. Magn.* 42 (11) (2006) 3674–3681.
- [31] J. G. Zhu, Numerical modelling of magnetic materials for computer aided design of electromagnetic devices, Ph.D. Dissertation, School of Electrical Engineering, University of Technology Sydney, Australia, July 1994.
- [32] H. R. Dakua, "Exchange bias and training effect in an amorphous Zn-Fe-O/nanocrystalline GaFeO<sub>3</sub> bilayer thin film," *Mater. Res. Bull.* 136 (2021) 111146.
- [33] Q. Yang, Z. Zhou, N.X. Sun, and M. Liu, "Perspectives of voltage control for magnetic exchange bias in multiferroic heterostructures," *Phys. Lett. A.* 381 (14) (2017) 1213–1222.